Inorganic Chemistry
Article

Inorg. Chem. **2010**, *49*, 199–208 **199**
DOI: 10.1021/ic901741n

Mn_7 and Mn_{12} Clusters From Use of 2-(Pyridine-2-yl)propan-2-ol: A New Half-Integer Single-Molecule Magnet

Taketo Taguchi,[†] Wolfgang Wernsdorfer,[‡] Khalil A. Abboud,[†] and George Christou*[,†]

[†]*Department of Chemistry, University of Florida, Gainesville, Florida 32611-7200, and* [‡]*Institut Néel, CNRS and Université J. Fournier, BP 166, 38042 Grenoble Cedex 9, France*

Received September 1, 2009

The syntheses, crystal structures, and magnetochemical characterization are reported for two new Mn clusters, $[Mn_7O_3(OH)_3(O_2CBu^t)_7(dmhmp)_4]$ (**1**) and $[Mn_{12}O_7(OH)(OMe)_2(O_2CPh)_{12}(dmhmp)_4(H_2O)]$ (**2**). They were obtained from the use of 2-(pyridine-2-yl)propan-2-ol (dmhmpH), a more bulky version of the 2-(hydroxymethyl)pyridine (hmpH) reagent commonly employed previously in Mn chemistry. The reaction of dmhmpH with $MnCl_2 \cdot 4H_2O$ and NaO_2CBu^t in MeCN/MeOH led to the heptanuclear complex **1**, whereas the analogous reaction with $Mn(O_2CPh)_2$ gave dodecanuclear complex **2**. Complexes **1** and **2** are both mixed-valent and are of unprecedented structural types. Complex **1** (Mn^{II}, $6Mn^{III}$) can be described as the fusion of butterfly-like $[Mn_4(\mu_3\text{-}O)_2]$ and tetrahedral $[Mn_4(\mu_4\text{-}O)]$ units by the sharing of a common Mn atom. Complex **2** ($3Mn^{II}$, $9Mn^{III}$) possesses a central $[Mn_4O_6]$ face-sharing incomplete dicubane, on either side of which is a tetrahedral $[Mn_4(\mu_4\text{-}O)]$ unit attached to the oxide ions of the former. Solid-state dc and ac magnetic susceptibility measurements on **1** and **2** establish that they possess unusual $S = 7/2$ and 13/2 ground states, respectively. The ac susceptibility studies on **2** revealed nonzero frequency-dependent out-of-phase (χ_M'') signals at temperatures below 3 K, indicating a single-molecule magnet (SMM). Magnetization versus applied dc field sweeps on single crystals of $\mathbf{2} \cdot 3CH_2Cl_2$ down to 0.04 K exhibited hysteresis, thus confirming complex **2** to be a new half-integer SMM.

Introduction

The synthesis and characterization of 3d metal clusters with various nuclearities and metal topologies continue to be of great interest for their fascinating physical properties as well as the intrinsic architectural beauty and aesthetically pleasing structures they often possess.[1] In particular, our group has been very interested in paramagnetic Mn^{III}-containing clusters because they often have a large ground state spin (S) and easy-axis-type magnetic anisotropy, giving a significant energy barrier to reversal of the magnetization vector. Thus, at sufficiently low temperatures, they function as nanoscale magnetic particles, and they therefore represent a molecular approach to nanomagnetism[2,3] Such single-molecule magnets (SMMs) not only exhibit hysteresis in magnetization versus dc field scans, the diagnostic property of a classical magnet, but also fascinating quantum mechanical properties such as quantum tunneling of magnetization (QTM)[4] and quantum phase interference.[5] Many different types of SMMs are now known,[6−8] and the majority continue to be in Mn clusters containing at least some Mn^{III} atoms, since the Jahn−Teller distortion of this high-spin d^4 in octahedral geometry is a source of significant single-ion axial anisotropy of the easy-axis type (as gauged by a negative axial

*To whom correspondence should be addressed. Tel.: +1-352-392-8314. Fax: +1-352-392-8757. E-mail: christou@chem.ufl.edu.

(1) Wang, X. J.; Langetepe, T.; Persau, C.; Kang, B.-S.; Sheldrick, G. M.; Fenske, D. *Angew. Chem., Int. Ed.* **2002**, *41*, 3818.

(2) (a) Bircher, R.; Chaboussant, G.; Dobe, D.; Güdel, H. U.; Oshsenbein, S. T.; Sieber, A.; Waldmann, O. *Adv. Funct. Mater.* **2006**, *16*, 209. (b) Gatteschi, D.; Sessoli, R. *Angew. Chem., Int. Ed.* **2003**, *42*, 268. (c) Oshio, H.; Nakano, M. *Chem.—Eur. J.* **2005**, *11*, 5178.

(3) (a) Bagai, R; Christou, G. *Chem. Soc. Rev.*, **2009**, *38* (4), 1011 and references therein. (b) Christou, G.; Gatteschi, D.; Hendrickson, D. N., Sessoli, R. *MRS Bull.* **2000**, *25*, 66 and references cited therein.

(4) (a) Friedman, J. R.; Sarachik, M. P.; Tejada, J.; Ziolo, R. *Phys. Rev. Lett.* **1996**, *76*, 3830. (b) Thomas, L.; Lionti, L.; Ballou, R.; Gatteschi, D.; Sessoli, R.; Barbara, B. *Nature* **1996**, *383*, 145.

(5) (a) Wernsdorfer, W.; Sessoli, R. *Science* **1999**, *284*, 133. (b) Wernsdorfer, W.; Soler, M.; Christou, G.; Hendrickson, D. N. *J. Appl. Phys.* **2002**, *91*, 7164. (c) Wernsdorfer, W.; Chakov, N. E.; Christou, G. *Phys. Rev. Lett.* **2005**, *95*, 037203.

(6) (a) Sessoli, R.; Gatteschi, D.; Caneschi, A.; Novak, M. A. *Nature* **1993**, *365*, 141. (b) Sessoli, R.; Tsai, H.-L.; Schake, A. R.; Wang, S.; Vincent, J. B.; Folting, K.; Gatteschi, D.; Christou, G.; Hendrickson, D. N. *J. Am. Chem. Soc.* **1993**, *115*, 1804.

(7) For example, see: (a) Gatteschi, D.; Sessoli, R.; Cornia, A. *Chem. Commun.* **2000**, 725. (b) Sun, Z. M.; Grant, C. M.; Castro, S. L.; Hendrickson, D. N.; Christou, G. *Chem. Commun.* **1998**, 721. (c) Yang, E. C.; Hendrickson, D. N.; Wernsdorfer, W.; Nakano, M.; Zakharov, L. N.; Sommer, R. D.; Rheingold, A. L.; Ledezma-Gairaud, M.; Christou, G. *J. Appl. Phys.* **2002**, *91*, 7382.

(8) (a) Andres, H.; Basler, R.; Blake, A. J.; Cadiou, C.; Chaboussant, G.; Grant, C. M.; Gudel, H. U.; Murrie, M.; Parsons, S.; Paulsen, C.; Semadini, F.; Villar, V.; Wernsdorfer, W.; Winpenny, R. E. P. *Chem.—Eur. J.* **2002**, *8*, 4867. (b) Murugesu, M.; Mishra, A.; Wernsdorfer, W.; Abboud, K. A.; Christou, G. *Polyhedron* **2006**, *25*, 613.

Published on Web 12/04/2009

zero-field splitting parameter, D) and thus of resulting anisotropy for the multinuclear molecular cluster. In addition, Mn clusters will often possess large ground state S values, the other requirement for a SMM, with the upper limit to the magnetization relaxation being given by $S^2|D|$ to second order.[3]

As a result of the above, there is a continuing need for new synthetic methods that can yield new polynuclear Mn/O complexes and new SMMs. In the development of new synthetic routes to metal clusters, the choice of the ligands is always a key issue. We and others have explored a wide variety of potentially chelating and bridging ligands that might foster the formation of high nuclearity products, and many interesting new clusters have been obtained. Examples include aliphatic or aromatic alcohols,[9−17] alcohol amines,[18−22] di-2-pyridylketone,[23−26] pyridyl-alcohols,[27,28] pyridyl ketone oximes,[29−33] salicylaldoximes,[34−39] and others.[40,42,43] As part of such efforts, we recently initiated a project in which the steric bulk of a given chelating/bridging ligand was increased by the addition of bulky groups at positions that we expect to influence the identity of the obtained cluster products. We chose for this work to modify the pyridyl-alcohol,

(9) (a) Milios, C. J.; Manoli, M.; Rajaraman, G.; Mishra, A.; Budd, L. E.; White, F.; Parsons, S.; Wernsdorfer, W.; Christou, G.; Brechin, E. K. *Inorg. Chem.* **2006**, *45*, 6782. (b) Manoli, M.; Prescimone, A.; Bagai, R.; Mishra, A.; Murugesu, M.; Parsons, S.; Wernsdorfer, W.; Christou, G.; Brechin, E. K. *Inorg. Chem.* **2007**, *46*, 6968.

(10) (a) Murugesu, M.; Wernsdorfer, W.; Abboud, K. A.; Brechin, E. K.; Christou, G. *Dalton Trans.* **2006**, 2285. (b) Manoli, M.; Milios, C. J.; Mishra, A.; Christou, G.; Brechin, E. K. *Polyhedron* **2007**, *26*, 1923.

(11) (a) Brechin, E. K.; Soler, M.; Christou, G.; Davidson, J.; Hendrickson, D. N.; Parsons, S.; Wernsdorfer, W. *Polyhedron* **2003**, *22*, 1771. (b) Piligkos, S.; Rajaraman, G.; Soler, M.; Kirchner, N.; van Slageren, J.; Bircher, R.; Parsons, S.; Gudel, H. U.; Kortus, J.; Wernsdorfer, W.; Christou, G.; Brechin, E. K. *J. Am. Chem. Soc.* **2005**, *127*, 5572. (c) Murugesu, M.; Wernsdorfer, W.; Christou, G.; Brechin, E. K. *Polyhedron* **2007**, *26*, 1845.

(12) (a) Brechin, E. K.; Soler, M.; Christou, G.; Helliwell, M.; Teat, S. J.; Wernsdorfer, W. *Chem. Commun.* **2003**, 1276. (b) Rajaraman, G.; Murugesu, M.; Sanudo, E. C.; Soler, M.; Wernsdorfer, W.; Helliwell, M.; Muryn, C.; Raftery, J.; Teat, S. J.; Christou, G.; Brechin, E. K. *J. Am. Chem. Soc.* **2004**, *126*, 15445. (c) Manoli, M.; Prescimone, A.; Mishra, A.; Parsons, S.; Christou, G.; Brechin, E. K. *Dalton Trans.* **2007**, 532.

(13) (a) Scott, R. T. W.; Parsons, S.; Murugesu, M.; Wernsdorfer, W.; Christou, G.; Brechin, E. K. *Angew. Chem., Int. Ed.* **2005**, *44*, 6540. (b) Milios, C. J.; Fabbiani, F. P. A.; Parsons, S.; Murugesu, M.; Christou, G.; Brechin, E. K. *Dalton Trans.* **2006**, 351. (c) Scott, R. T. W.; Milios, C. J.; Vinslava, A.; Lifford, D.; Parsons, S.; Wernsdorfer, W.; Christou, G.; Brechin, E. K. *Dalton Trans.* **2006**, 3161.

(14) Moushi, E. E.; Stamatatos, Th. C.; Wernsdorfer, W.; Nastopoulos, V.; Christou, G.; Tasiopoulos, A. J. *Inorg. Chem.* **2009**, *48*, 5049.

(15) (a) Moushi, E. E.; Stamatatos, T. C.; Wernsdorfer, W.; Nastopoulos, V.; Christou, G.; Tasiopoulos, A. J. *Angew. Chem., Int. Ed.* **2006**, *45*, 7722. (b) Nayak, S.; Lan, Y.; Clérac, R.; Ansona, C. E.; Powell, A. K. *Chem. Commun.* **2008**, 5698.

(16) Ako, A. M.; Hewitt, I. J; Mereacre, V.; Clérac, R.; Wernsdorfer, W.; Anson, C. E.; Powell, A. K. *Angew. Chem., Int. Ed.* **2006**, *45*, 4926.

(17) (a) Aromi, G.; Gamez, P.; Roubeau, O.; Berzal, P. C.; Kooijman, H.; Spek, A. L.; Driessen, W. L.; Reedijk, J. *Inorg. Chem.* **2002**, *41*, 3673. (b) Yang, C.-I.; Lee, G.-H.; Wur, C.-S.; Lin, J. G.; Tsai, H.-L. *Polyhedron* **2005**, *24*, 2215.

(18) (a) Foguet-Albiol, D.; O'Brien, T. A.; Wernsdorfer, W.; Moulton, B.; Zaworotko, M. J.; Abboud, K. A.; Christou, G. *Angew. Chem., Int. Ed.* **2005**, *44*, 897. (b) Rumberger, E. M.; Shah, S. J.; Beedle, C. C.; Zakharov, L. N.; Rheingold, A. L.; Hendrickson, D. N. *Inorg. Chem.* **2005**, *44*, 2742.

(19) (a) Saalfrank, R. W.; Nakajima, T.; Mooren, N.; Scheurer, A.; Maid, H.; Hampel, F.; Trieflinger, C.; Daub, J. *Eur. J. Inorg. Chem.* **2005**, 1149. (b) Saalfrank, R. W.; Prakash, R.; Maid, H.; Hampel, F.; Heinemann, F. W.; Trautwein, A. X.; Bottger, L. H. *Chem.—Eur. J.* **2006**, *12*, 2428. (c) Saalfrank, R. W.; Scheurer, A.; Prakash, R.; Heinemann, F. W.; Nakajima, T.; Hampel, F.; Leppin, R.; Pilawa, B.; Rupp, H.; Muller, P. *Inorg. Chem.* **2007**, *46*, 1586.

(20) (a) Ako, A. M.; Mereacre, V.; Hewitt, I. J.; Clerac, R.; Lecren, L.; Anson, C. E.; Powell, A. K. *J. Mater. Chem.* **2006**, *16*, 2579. (b) Liu, T.; Wang, B.-W.; Chen, Y.-H.; Wang, Z.-M.; Gao, S. *Z. Anorg. Allg. Chem.* **2008**, *634*, 778.

(21) (a) Murugesu, M.; Wernsdorfer, W.; Abboud, K. A.; Christou, G. *Angew. Chem., Int. Ed.* **2005**, *44*, 892. (b) Beedle, C. C.; Heroux, K. J.; Nakano, M.; DiPasquale, A. G.; Rheingold, A. L.; Hendrickson, D. N. *Polyhedron* **2007**, *26*, 2200.

(22) (a) Wittick, L. M.; Jones, L. F.; Jensen, P.; Moubaraki, B.; Spiccia, L.; Berry, K. J.; Murray, K. S. *Dalton Trans.* **2006**, 1534. (b) Wittick, L. M.; Murray, K. S.; Moubaraki, B.; Batten, S. R.; Spiccia, L.; Berry, K. J. *Dalton Trans.* **2004**, 1003.

(23) (a) Milios, C. J.; Kefalloniti, E.; Raptopoulou, C. P.; Terzis, A.; Vicente, R.; Lalioti, N.; Escuer, A.; Perlepes, S. P. *Chem. Commun.* **2003**, 819. (b) Milios, C. J.; Kyritsis, P.; Raptopoulou, C. P.; Terzis, A.; Vicente, R.; Escuer, A.; Perlepes, S. P. *Dalton Trans.* **2005**, 501.

(24) (a) Papaefstathiou, G. S.; Escuer, A.; Raptopoulou, C. P.; Terzis, A.; Perlepes, S. P.; Vicente, R. *Eur. J. Inorg. Chem.* **2001**, 1567. (b) Papaefstathiou, G. S.; Escuer, A.; Mautner, F. A.; Raptopoulou, C.; Terzis, A.; Perlepes, S. P.; Vicente, R. *Eur. J. Inorg. Chem.* **2005**, 879. (c) Stoumpos, C. C.; Gass, I. A.; Milios, C. J.; Kefalloniti, E.; Raptopoulou, C. P.; Terzis, A.; Lalioti, N.; Brechin, E. K.; Perlepes, S. P. *Inorg. Chem. Commun.* **2008**, *11*, 196.

(25) (a) Zaleski, C. M.; Depperman, E. C.; Dendrinou-Samara, C.; Alexiou, M.; Kampf, J. W.; Kessissoglou, D. P.; Kirk, M. L.; Pecoraro, V. L. *J. Am. Chem. Soc.* **2005**, *127*, 12862. (b) Dendrinou-Samara, C.; Alexiou, M.; Zaleski, C. M.; Kampf, J. W.; Kirk, M. L.; Kessissoglou, D. P.; Pecoraro, V. L. *Angew. Chem., Int. Ed.* **2003**, *42*, 3763. (c) Stamatatos, Th. C.; Abboud, K. A.; Wernsdorfer, W.; Christou, G. *Angew. Chem., Int. Ed.* **2008**, *47*, 6694.

(26) (a) Tong, M.-L.; Lee, H. K.; Zheng, S.-L.; Chen, X.-M. *Chem. Lett.* **1999**, 1087. (b) Tong, M.-L.; Zheng, S.-L.; Shi, J.-X.; Tong, Y.-X.; Lee, H. K.; Chen, X.-M. *J. Chem. Soc., Dalton Trans.* **2002**, 1727.

(27) (a) Harden, N. C.; Bolcar, M. A.; Wernsdorfer, W.; Abboud, K. A.; Streib, W. E.; Christou, G. *Inorg. Chem.* **2003**, *42*, 7067. (b) Boskovic, C.; Brechin, E.; Streib, W. E.; Folting, K.; Bollinger, J. C.; Hendrickson, D. N.; Christou, G. *J. Am. Chem. Soc.* **2002**, *124*, 3725. (c) Stamatatos, Th. C.; Abboud, K. A.; Wernsdorfer, W.; Christou, G. *Angew. Chem., Int. Ed.* **2006**, *45*, 4134.

(28) (a) Murugesu, M.; Habrych, M.; Wernsdorfer, W.; Abboud, K. A.; Christou, G. *J. Am. Chem. Soc.* **2004**, *126*, 4766. (b) Boskovic, C.; Wernsdorfer, W.; Folting, K.; Huffman, J. C.; Hendrickson, D. N.; Christou, G. *Inorg. Chem.* **2002**, *41*, 5107. (c) Brechin, E. K.; Yoo, J.; Huffman, J. C.; Hendrickson, D. N.; Christou, G. *Chem. Commun.* **1999**, 783.

(29) (a) Stamatatos, Th. C.; Foguet-Albiol, D.; Lee, S. C.; Stoumpos, C. C.; Raptopoulou, C. P.; Terzis, A.; Wernsdorfer, W.; Hill, S.; Perlepes, S. P.; Christou, G. *J. Am. Chem. Soc.* **2007**, *129*, 9484. (b) Stamatatos, T. C.; Luisi, B. S.; Moulton, B.; Christou, G. *Inorg. Chem.* **2008**, *47*, 1134.

(30) (a) Milios, C. J.; Kefalloniti, E.; Raptopoulou, C. P.; Terzis, A.; Escuer, A.; Vicente, R.; Perlepes, S. P. *Polyhedron* **2004**, *23*, 83. (b) Milios, C. J.; Stamatatos, T. C.; Kyritsis, P.; Terzis, A.; Raptopoulou, C. P.; Vicente, R.; Escuer, A.; Perlepes, S. P. *Eur. J. Inorg. Chem.* **2004**, 2885. (c) Milios, C. J.; Piligkos, S.; Bell, A. R.; Laye, R. H.; Teat, S. J.; Vicente, R.; McInnes, E.; Escuer, A.; Perlepes, S. P.; Winpenny, R. E. P. *Inorg. Chem. Commun.* **2006**, *9*, 638.

(31) (a) Dendrinou-Samara, C.; Zaleski, C. M.; Evagorou, A.; Kampf, J. W.; Pecoraro, V. L.; Kessissoglou, D. P. *Chem.Commun.* **2003**, 2668. (b) Alexiou, M.; Zaleski, C. M.; Dendrinou-Samara, C.; Kampf, J.; Kessissoglou, D. P.; Pecoraro, V. L. *Z. Anorg. Allg. Chem.* **2003**, *629*, 2348.

(32) (a) Alexiou, M.; Dendrinou-Samara, C.; Karagianni, A.; Biswas, S.; Zaleski, C. M.; Kampf, J.; Yoder, D.; Penner-Hahn, J. E.; Pecoraro, V. L.; Kessissoglou, D. P. *Inorg. Chem.* **2003**, *42*, 2185. (b) Psomas, G.; Stemmler, A. J.; Dendrinou-Samara, C.; Bodwin, J. J.; Schneider, M.; Alexiou, M.; Kampf, J. W.; Kessissoglou, D. P.; Pecoraro, V. L. *Inorg. Chem.* **2001**, *40*, 1562.

(33) (a) Roubeau, O.; Lecren, L.; Li, Y.-G.; Le Goff, X. F.; Clerac, R. *Inorg. Chem. Commun.* **2005**, *8*, 314. (b) Dimitrakopoulou, A.; Dendrinou-Samara, C.; Pantazaki, A. A.; Alexiou, M.; Nordlander, E.; Kessissoglou, D. P. *J. Inorg. Biochem.* **2008**, *102*, 618. (c) Papatriantafyllopoulou, C.; Raptopoulou, C. P.; Escuer, A.; Milios, C. J. *Inorg. Chim. Acta* **2007**, *360*, 61.

(34) (a) Milios, C. J.; Vinslava, A.; Wernsdorfer, W.; Prescimone, A.; Wood, P. A.; Parsons, S.; Perlepes, S. P.; Christou, G.; Brechin, E. K. *J. Am. Chem. Soc.* **2007**, *129*, 6547. (b) Milios, C. J.; Inglis, R.; Vinslava, A.; Bagai, R.; Wernsdorfer, W.; Parsons, S.; Perlepes, S. P.; Christou, G.; Brechin, E. K. *J. Am. Chem. Soc.* **2007**, *129*, 12505.

(35) Milios, C. J.; Gass, I. A.; Vinslava, A.; Budd, L.; Parsons, S.; Wernsdorfer, W.; Perlepes, S. P.; Christou, G.; Brechin, E. K. *Inorg. Chem.* **2007**, *46*, 6215 and references therein.

(36) Milios, C. J.; Vinslava, A.; Wood, P. A.; Parsons, S.; Wernsdorfer, W.; Christou, G.; Perlepes, S. P.; Brechin, E. K. *J. Am. Chem. Soc.* **2007**, *129*, 8.

(37) (a) Milios, C. J.; Vinslava, A.; Whittaker, A. G.; Parsons, S.; Wernsdorfer, W.; Christou, G.; Perlepes, S. P.; Brechin, E. K. *Inorg. Chem.* **2006**, *45*, 5272. (b) Milios, C. J.; Raptopoulou, C. P.; Terzis, A.; Lloret, F.; Vicente, R.; Perlepes, S. P.; Escuer, A. *Angew. Chem., Int. Ed.* **2004**, *43*, 210.

2-(hydroxymethyl)pyridine (hmpH), and recently reported the use in Mn cluster chemistry of the derivative with two phenyl groups substituted at the CH_2 position, that is, diphenyl-hmpH (dphmpH; IUPAC name is diphenyl(pyridine-2-yl)methanol; Scheme 1). The Mn_4, Mn_6, and Mn_{11} products obtained with dphmpH were different, as hoped, from those obtained previously with hmpH, and we also saw that $dphmp^-$ prefers to bind as a bidentate chelate, disfavoring the bridging modes favored by hmp^-.[44] We thus decided to change the substituents to ones that might switch back on the bridging modes while still hopefully giving different products than hmpH and chose to employ dimethyl-hmpH (dmhmpH; IUPAC name is 2-(pyridine-2-yl)propan-2-ol; Scheme 1). Note that dmhmpH has been employed previously only to prepare mononuclear complexes of V, Zr, Mo, and W and dinuclear complexes of Ni and W.[45,46] We deliberately targeted higher-nuclearity Mn_x products and have successfully isolated new Mn_7 and Mn_{12} complexes with prototypical metal topologies. The syntheses, structures, and magnetochemical characterization of these complexes are described herein.

Experimental Section

Syntheses. All preparations were performed under aerobic conditions except for the synthesis of dmhmpH, which was carried out as previously reported.[47] All chemicals were used as received.

$[Mn_7O_3(OH)_3(O_2CBu^t)_7(dmhmp)_4]$ (1). To a stirred solution of dmhmpH (0.14 g, 1.00 mmol) and NEt_3 (0.14 mL, 1.0 mmol) in MeCN/MeOH (27 mL, 25:2 v/v) was added solid $MnCl_2 \cdot 4H_2O$ (0.20 g, 1.0 mmol) and $NaO_2C^tBu \cdot H_2O$ (0.25 g, 2.0 mmol). The mixture was stirred overnight, filtered to remove NaCl, and the filtrate left undisturbed to concentrate slowly by evaporation. X-ray-quality crystals of $1 \cdot 7MeCN$ slowly grew over 2 weeks, and they were collected by filtration, washed with cold MeCN (2×5 mL), and dried under a vacuum. The yield was 50%. The vacuum-dried solid was analyzed as $1 \cdot MeCN$.

Scheme 1

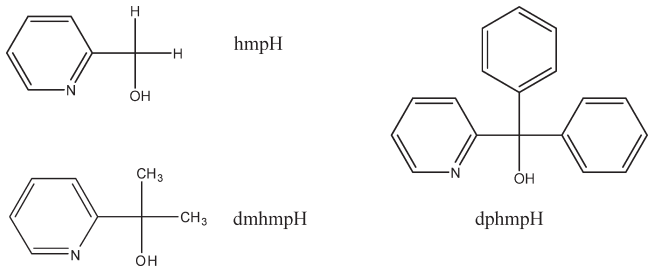

Anal. Calcd (Found) for $C_{69}H_{113}N_5Mn_7O_{24}$: C, 46.53 (46.93); H, 6.39 (6.32); N, 3.93 (3.51). Selected IR data (cm^{-1}): 3423(wb), 2956(m), 2926(w), 2868(w), 1595(s), 1545(s), 1482(s), 1458(w), 1415(s), 1358(s), 1277(w), 1225(w), 1181(m), 1123(m), 1101(w), 1502(w), 1032(w), 982(m), 889(w), 782(m), 757(w), 741(w), 661(s), 611(m), 563(m), 516(w), 436(w).

$[Mn_{12}O_7(OH)(OMe)_2(O_2CPh)_{12}(dmhmp)_4(H_2O)]$ (2) Method A. To a stirred solution of dmhmpH (0.14 g, 1.0 mmol) and NEt_3 (0.42 mL, 3.0 mmol) in CH_2Cl_2/MeOH (31 mL, 30:1 v/v) was added solid $Mn(O_2CPh)_2$ (0.33 g, 1.0 mmol). The resulting dark brown solution was stirred overnight and filtered and the filtrate carefully layered with Et_2O (60 mL). X-ray-quality crystals of $2 \cdot 3CH_2Cl_2$ slowly grew over 2 weeks, and they were collected by filtration, washed with Et_2O (2×5 mL), and dried under a vacuum. The yield was 55%. The vacuum-dried solid was slightly hygroscopic and analyzed as $2 \cdot 3H_2O$. Anal. Calcd (Found) for $C_{118}H_{119}N_4Mn_{12}O_{42}$: C, 48.46 (48.34); H, 4.10 (3.84); N, 1.92 (1.83). Selected IR data (cm^{-1}): 3434(mb), 3063(w), 2974(m), 2922(m), 2813(w), 1603(s), 1565(s), 1483(m), 1401(s), 1305(w), 1278(w), 1252(w), 1180(m), 1123(m), 1101(w), 1067(w), 1052(m), 1027(m), 978(m), 936(w), 885(w), 839(w), 816(w), 782(m), 717(s), 667(s), 620(s), 557(s), 463(m), 433(m).

Method B. To a stirred solution of dmhmpH (0.14 g, 1.0 mmol) and NEt_3 (0.42 mL, 3.0 mmol) in MeCN/MeOH (30 mL, 5:1 v/v) was added solid $Mn(O_2CPh)_2$ (0.33 g, 1.0 mmol). The resulting dark brown solution was stirred for 3 h and filtered and the filtrate left undisturbed at ambient temperature. Brown crystals were obtained after 3 days, and these were collected by filtration, washed with cold MeCN (2×3 mL) and Et_2O (2×5 mL), and dried under a vacuum. The yield was 45%. The product was identified by IR spectral comparison with material from Method A.

X-Ray Crystallography. Data were collected on a Siemens SMART PLATFORM equipped with a CCD area detector and a graphite monochromator utilizing Mo Kα radiation (λ = 0.71073 Å). Suitable crystals of $1 \cdot 7MeCN$ and $2 \cdot 3CH_2Cl_2$ were attached to glass fibers using silicone grease and transferred to a goniostat where they were cooled to 173 K for data collection. Cell parameters were refined using up to 8192 reflections. A full sphere of data (1850 frames) was collected using the ω-scan method (0.3° frame width). The first 50 frames were remeasured at the end of data collection to monitor instrument and crystal stability (maximum correction on I was < 1%). Absorption corrections by integration were applied on the basis of measured indexed crystal faces. The structure was solved by the direct methods in SHELXTL6[48] and refined on F^2 using full-matrix least squares. The non-H atoms were refined anisotropically, except where stated, whereas the H atoms were placed in calculated, ideal positions and refined as riding on their respective C atoms.

For $1 \cdot 7MeCN$, the asymmetric unit consists of a Mn_7 cluster and seven MeCN molecules. The latter were disordered and could not be modeled properly; thus, the program SQUEEZE,[49] a part of the PLATON package of crystallographic software, was used to calculate the solvent disorder area and remove its

(38) (a) Chaudhuri, P.; Birkelbach, F.; Winter, M.; Staemmler, V.; Fleischhauer, P.; Haase, W.; Florke, U.; Haupt, H.-J. *J. Chem. Soc., Dalton Trans.* **1994**, 2313. (b) Chaudhuri, P.; Rentschler, E.; Birkelbach, F.; Krebs, C.; Bill, E.; Weyhermuller, T.; Florke, U. *Eur. J. Inorg. Chem.* **2003**, 541.

(39) (a) Xu, H.-B.; Wang, B.-W.; Pan, F.; Wang, Z.-M.; Gao, S. *Angew. Chem., Int. Ed.* **2007**, *46*, 7388. (b) Yang, C.-I.; Wernsdorfer, W.; Lee, G.-H.; Tsai, H.-L. *J. Am. Chem. Soc.* **2007**, *129*, 456.

(40) (a) Zhou, A.-J.; Qin, L.-J.; Beedle, C. C.; Ding, S.; Nakano, M.; Leng, J.-D.; Tong, M.-L.; Hendrickson, D. N. *Inorg. Chem.* **2007**, *46*, 8111. (b) Bagai, R.; Abboud, K. A.; Christou, G. *Inorg. Chem.* **2008**, *47*, 621.

(41) (a) Koizumi, S.; Nihei, M.; Nakano, M.; Oshio, H. *Inorg. Chem.* **2005**, *44*, 1208. (b) Koizumi, S.; Nihei, M.; Shiga, T.; Nakano, M.; Nojiri, H.; Bircher, R.; Waldmann, O.; Ochsenbein, S. T.; Gudel, H. U.; Fernandez-Alonso, F.; Oshio, H. *Chem.—Eur. J.* **2007**, *13*, 8445.

(42) (a) Gibney, B. R.; Wang, H.; Kampf, J. W.; Pecoraro, V. L. *Inorg. Chem.* **1996**, *35*, 6184. (b) Kessissoglou, D. P.; Bodwin, J. J.; Kampf, J.; Dendrinou-Samara, C.; Pecoraro, V. L. *Inorg. Chim. Acta* **2002**, *331*, 73.

(43) (a) Kessissoglou, D. P.; Kampf, J.; Pecoraro, V. L. *Polyhedron* **1994**, *13*, 1379. (b) Aromi, G.; Bell, A.; Teat, S. J.; Whittaker, A. G.; Winpenny, R. E. P. *Chem.Commun.* **2002**, 1896. (c) Sañudo, E. C.; Wernsdorfer, W.; Abboud, K. A.; Christou, G. *Inorg. Chem.* **2004**, *43*, 4137.

(44) Taguchi, T; Daniels, M. R.; Abboud, K. A.; Christou, G. *Inorg. Chem.* **2009**, *48*, 9325.

(45) (a) Hagen, H.; Bezemer, C.; Boersma, J.; Kooijman, H.; Lutz, M.; Spek, A. L.; Van Koten, G. *Inorg. Chem.* **2000**, *39*, 3970. (b) Tsukahara, T.; Swenson, D. C.; Jordan, R. F. *Organometallics* **1997**, *16*, 3303. (c) Brandts, J. A. M.; Boersma, J.; Spek, A. L.; van Koten, G. *Eur. J. Inorg. Chem.* **1999**, 1727. (d) Herrmann, W. A.; Fridgen, J.; Lobmaier, G. M.; Spiegler, M. *New J. Chem.* **1999**, *23*, 5. (e) Hayton, T. W.; Boncella, J. M.; Scott, B. L.; Abboud, K. A.; Mills, R. C. *Inorg. Chem.* **2005**, *44*, 9506.

(46) (a) Speiser, F.; Braunstein, P.; Saussine, L. *Inorg. Chem.* **2004**, *43*, 4234. (b) Coutelier, O.; Gauvin, R. M.; Nowogrocki, G.; Trebosc, J.; Delevoye, L.; Mortreux, A. *Eur. J. Inorg. Chem.* **2007**, 5541.

(47) Ridd, M. J.; Gakowski, D. J.; Sneddon, G. E.; Keene, F. R. *J. Chem. Soc., Dalton Trans.* **1992**, 1949.

(48) *SHELXTL6*; Bruker-AXS: Madison, WI, 2000.

(49) Van der Sluis, P.; Spek, A. L. *Acta Crystallogr., Sect. A* **1990**, *A46*, 194.

contribution to the overall intensity data. The pivalate groups on carboxylate C atoms C48 and C63 were rotationally disordered, and the Me C atoms refined isotropically at two positions with 65/35% and 57/43% occupancies, respectively. The three protons H4, H5, and H6 on O4, O5, and O6 were obtained from a difference Fourier map; H4 and H6 were refined freely, but H5 was refined as riding on O5. A total of 915 parameters were refined in the final cycle of refinement using 14 701 reflections with $I > 2\sigma(I)$ to yield an R_1 and wR_2 of 8.59 and 16.20%, respectively.

For $\mathbf{2}\cdot 3CH_2Cl_2$, the asymmetric unit consists of a Mn_{12} cluster and three disordered CH_2Cl_2 molecules. The latter were disordered and could not be modeled properly; thus, the program SQUEEZE was again used to calculate the solvent disorder area and remove its contribution to the overall intensity data. The benzoate ligands at C atoms C81 and C91 are disordered, and each was refined in two positions with their site occupation factors fixed at 0.5 (after refining to near 50%). The phenyl rings of the disordered benzoates were idealized to a hexagonal shape. A total of 30 912 parameters were refined in the final cycle of refinement using 16 954 reflections with $I > 2\sigma(I)$ to yield a R_1 and wR_2 of 4.19 and 11.64%, respectively.

Unit cell data and details of the structure refinements for the two complexes are listed in Table 1.

Other Studies. Infrared spectra were recorded in the solid state (KBr pellets) on a Nicolet Nexus 670 FTIR spectrometer in the 400−4000 cm^{-1} range. Elemental analyses (C, H, and N) were performed by the in-house facilities of the University of Florida, Chemistry Department. Variable-temperature dc and ac magnetic susceptibility data were collected on vacuum-dried solids using a Quantum Design MPMS-XL SQUID susceptometer equipped with a 7 T magnet and operating in the 1.8−300 K range. Samples were embedded in solid eicosane to prevent torquing. Magnetization versus field and temperature data were fit using the program MAGNET. Pascal's constants[50] were used to estimate the diamagnetic correction, which was subtracted from the experimental susceptibility to give the molar paramagnetic susceptibility (χ_M).

Results and Discussion

Syntheses. A variety of reactions were explored with different Mn starting materials and under different reagent ratios, solvents, and other conditions before the following successful procedures were identified. The reaction of dmhmpH with $MnCl_2\cdot 4H_2O$, $NaO_2C^tBu\cdot H_2O$, and NEt_3 in a 1:1:2:1 ratio in MeCN/MeOH afforded a brown solution from which was subsequently isolated $[Mn_7O_3(OH)_3(O_2C^tBu)_7(dmhmp)_4]$ (**1**) in 50% yield. Its formation is summarized in eq 1, assuming atmospheric O_2 is the oxidizing agent. The mixed solvent system was needed to ensure adequate solubility of all reagents. Small variations in the Mn/dmhmpH/$^tBuCO_2^-$ ratio also gave complex **1**.

$$7Mn^{2+} + 4dmhmpH + 7Bu^tCO_2^- + 7NEt_3 + (3/2)O_2 + 3H_2O \rightarrow [Mn_7O_3(OH)_3(O_2CBu^t)_7(dmhmp)_4] + 7NHEt_3^+ \quad (1)$$

In our previous work with dphmpH, we found the identity of the product was dependent on the carboxylate employed, and we thus investigated this point with dmhmpH also. Indeed, the reaction of dmhmpH with

(50) Weast, R. C. *CRC Handbook of Chemistry and Physics*; CRC Press, Inc.: Boca Raton, FL, 1984.

Table 1. Crystallographic Data for $\mathbf{1}\cdot 7MeCN$ and $\mathbf{2}\cdot 3CH_2Cl_2$

	1	**2**
formula[a]	$C_{67}H_{106}Mn_7N_4O_{24}$	$C_{118}H_{108}Mn_{12}N_4O_{39}$
fw, g mol^{-1}[a]	1736.14	2865.36
cryst syst	triclinic	triclinic
space group	$P\bar{1}$	$P\bar{1}$
a, Å	14.396(3)	15.9055(12)
b, Å	15.169(3)	17.0160(13)
c, Å	25.551(6)	27.771(2)
α, deg	77.295(4)	107.1080(10)
β, deg	88.592(4)	99.8710(10)
γ, deg	63.557(3)	108.4790(10)
V, Å^3	4856.3(18)	6516.3(9)
Z	2	2
T, K	173(2)	173(2)
radiation, Å[b]	0.71073	0.71073
ρ_{calc}, g cm^{-3}	1.187	1.460
μ, mm^{-1}	0.940	1.197
R_{av}	0.0371	0.0326
R1[c,d]	0.0610	0.0419
wR2[e]	0.1538	0.1164

[a] Including solvate molecules. [b] Graphite monochromator. [c] $I > 2\sigma(I)$. [d] $R1 = \sum(|F_o| - |F_c|)/\sum F_o|$. [e] $wR2 = [\sum[w(F_o^2 - F_c^2)^2]/\sum[w(F_o^2)^2]]^{1/2}$, $w = 1/[\sigma^2(F_o^2) + [(ap)^2 + bp]$, where $p = [\max(F_o^2, 0) + 2F_c^2]/3$.

$Mn(O_2CPh)_2$ and NEt_3 in a 1:1:3 ratio in CH_2Cl_2/MeOH now gave as the isolated product the dodecanuclear complex $[Mn_{12}O_7(OH)(OMe)_2(O_2CPh)_{12}(dmhmp)_4(H_2O)]$ (**2**) in 55% yield (Method A). The same reaction in MeCN/MeOH also gave **2** but in a slightly lower yield of 45% (Method B). Its formation is summarized in eq 2.

$$12Mn(O_2CPh)_2 + 4dmhmpH + 17NEt_3 + (9/4)O_2 + (9/2)H_2O + 2MeOH \rightarrow [Mn_{12}O_7(OH)(OMe)_2(O_2CPh)_{12}(dmhmp)_4(H_2O)] + 12PhCO_2^- + 12NHEt_3^+ \quad (2)$$

It is clear that the reactions that lead to **1** and **2** are very complicated and involve acid/base and redox chemistry, and the reaction solutions likely contain a complicated mixture of several species in equilibrium. As a result, the isolated product will be sensitive to factors such as relative solubility and crystallization kinetics, and this rationalizes the fact that changing the carboxylate from pivalate to benzoate causes a major change in product. Along these lines, it is worth noting that the results here parallel those previously obtained with the bulkier dphmpH when used in otherwise identical reaction systems as those for **1** and **2**; the products were $[Mn_4O_2(O_2C^tBu)_5(dphmp)_3]$ and $[Mn_6O_4(OMe)_2(O_2CPh)_4(dphmp)_4]$ for pivalate and benzoate, respectively.[44]

Description of Structures. The structure and a stereoview of $[Mn_7O_3(OH)_3(O_2C^tBu)_7(dmhmp)_4]$ (**1**) are shown in Figure 1, and its labeled core in Figure S1 (Supporting Information). Selected interatomic distances and angles are listed in Table 2. The complex contains a $[Mn_7(\mu_4\text{-}O)(\mu_3\text{-}O)_2(\mu\text{-}O)_5]$ core comprising a $[Mn_4(\mu_3\text{-}O)_2]$ butterfly-like unit and a $[Mn_4(\mu_4\text{-}O)]$ tetrahedral unit fused at shared Mn atom Mn1. Note that the related $[Mn_4O_2]^{8+}$ butterfly complex $[Mn_4O_2(O_2CPh)_7(hmp)_2]^-$ has been

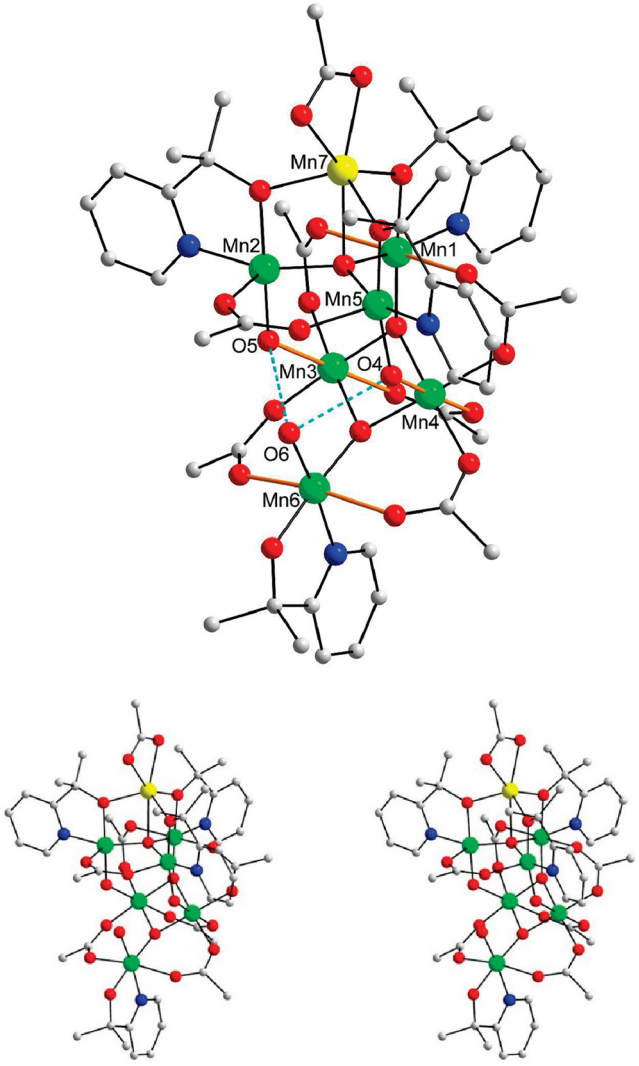

Figure 1. Structure of complex **1** with intramolecular H bonds shown as dashed lines (top) and a stereopair (bottom). The thicker orange bonds indicate the Mn^{III} Jahn−Teller elongation axes. H atoms and pivalate Me groups have been omitted for clarity. Color code: Mn^{II}, yellow; Mn^{III}, green; O, red; N, blue; C, gray.

obtained previously in discrete form[51] and has an hmp^- group chelating to each "wing-tip" Mn^{III} atom, as do two of the $dmhmp^-$ groups in **1**. One of the latter and the two other $dmhmp^-$ groups each bound in a $\eta^1{:}\eta^2{:}\mu$ mode, chelating to a Mn^{III} of the tetrahedral unit and bridging with their O atom to the Mn^{II} atom, Mn7. Two additional OH^- ions, O4 and O5, bridge between a "body" Mn atom (Mn3 or Mn4) and Mn2 or Mn5, respectively, of the tetrahedral unit. Ligation is completed by six $\eta^1{:}\eta^1{:}\mu$ pivalate groups bridging $Mn^{III}Mn^{III}$ pairs, a chelating pivalate on Mn^{II} atom Mn7, and a terminal OH^- ion (O6) on Mn6. Charge considerations, the metric parameters, and the presence of Mn^{III} Jahn−Teller (JT) distortions (axial elongations) indicate a $Mn^{II}Mn^{III}{}_6$ description, as confirmed by bond valence sum (BVS) calculations (Table 3).[52] BVS calculations were also performed on the inorganic O atoms to identify their degree of protonation and thus distinguish O^{2-}, OH^-, and H_2O situations (Table 4). These confirm three O^{2-} ions (one μ_4- and two μ_3-) and three OH^- ions (a terminal OH^- (O6) and two μ-OH^-, O4 and O5, ions). The BVS value of 0.63 for O6 is unusually low for a OH^- ion but is consistent with it acting as a double H-bond acceptor atom for two hydrogen bonds with μ-OH^- ions O4 and O5 (O4···O6 = 2.711(5) Å, O5···O6 = 2.767(5) Å). We have seen in the past a similarly unusual lowering of the BVS of an O atom

(51) Bouwman, E.; Bolcar, M. A.; Libby, E.; Huffman, J. C.; Folting, K.; Christou, G. *Inorg. Chem.* **1992**, *31*, 5185.
(52) (a) Brown, I. D.; Altermatt, D. *Acta Crystallogr.* **1985**, *B41*, 244. (b) Liu, W.; Thorp, H. H. *Inorg. Chem.* **1993**, *32*, 4102.

Table 2. Selected Interatomic Distances (Å) and Angles (deg) for **1**·7MeCN

Mn1−O1	1.866(2)	Mn4−O14	2.004(3)
Mn1−O7	1.887(2)	Mn4−O4	2.224(3)
Mn1−O2	1.895(2)	Mn4−O12	2.236(3)
Mn1−N1	2.015(3)	Mn5−O4	1.859(3)
Mn1−O15	2.263(3)	Mn5−O2	1.897(3)
Mn1−O13	2.303(3)	Mn5−O9	1.905(3)
Mn2−O5	1.867(2)	Mn5−N3	2.021(3)
Mn2−O8	1.899(3)	Mn5−O23	2.127(3)
Mn2−O2	1.910(3)	Mn5−O13	2.522(3)
Mn2−N2	2.031(3)	Mn6−O10	1.871(3)
Mn2−O24	2.110(3)	Mn6−O6	1.882(3)
Mn2−O15	2.588(3)	Mn6−O3	1.920(3)
Mn3−O3	1.889(3)	Mn6−N4	2.040(4)
Mn3−O1	1.916(2)	Mn6−O20	2.258(3)
Mn3−O21	1.946(3)	Mn6−O22	2.273(3)
Mn3−O16	1.973(3)	Mn7−O8	2.141(3)
Mn3−O5	2.206(3)	Mn7−O9	2.148(3)
Mn3−O11	2.254(3)	Mn7−O7	2.191(3)
Mn4−O1	1.893(3)	Mn7−O17	2.204(3)
Mn4−O3	1.899(3)	Mn7−O18	2.257(3)
Mn4−O19	1.941(3)	Mn7−O2	2.362(2)
Mn1−O1−Mn3	128.58(13)	Mn5−O2−Mn2	127.35(13)
Mn1−O1−Mn4	126.46(13)	Mn5−O2−Mn7	98.7(1)
Mn1−O2−Mn2	112.28(12)	Mn5−O4−Mn4	129.35(13)
Mn1−O2−Mn5	113.73(13)	Mn5−O9−Mn7	106.24(12)
Mn1−O2−Mn7	98.4(1)	Mn3−O3−Mn4	95.75(11)
Mn1−O7−Mn7	104.84(11)	Mn3−O3−Mn6	127.16(14)
Mn2−O2−Mn7	98.59(10)	Mn4−O3−Mn6	127.99(14)
Mn2−O5−Mn3	127.47(12)	Mn2−O8−Mn7	107.07(12)

Table 3. BVS for the Mn Atoms in **1** and **2**[a]

atom	Mn^{II}	Mn^{III}	Mn^{IV}
		1	
Mn1	3.32	3.07	3.06
Mn2	3.13	2.90	2.89
Mn3	3.13	2.86	3.01
Mn4	3.12	2.85	2.99
Mn5	3.16	2.93	2.92
Mn6	3.25	3.00	3.00
Mn7	1.80	1.65	1.73
		2	
Mn1	3.13	2.86	3.01
Mn2	3.17	2.90	3.05
Mn3	3.12	2.85	3.00
Mn4	3.20	2.93	3.07
Mn5	3.22	2.97	2.97
Mn6	1.87	1.71	1.80
Mn7	1.81	1.66	1.74
Mn8	3.27	3.02	3.02
Mn9	3.32	3.07	3.07
Mn10	3.26	3.01	3.01
Mn11	3.14	2.87	3.01
Mn12	1.92	1.76	1.84

[a] The underlined value is the one closest to the charge for which it was calculated; the nearest whole number can be taken as the oxidation state of that atom.

Table 4. BVS for Selected O Atoms in **1** and **2**[a]

atom	BVS	assgt
	1	
O1	1.85	O^{2-}
O2	1.98	O^{2-}
O3	1.79	O^{2-}
O4	0.93	OH^{-}
O5	0.93	OH^{-}
O6	0.63	OH^{-}
	2	
O1	1.75	O^{2-}
O2	1.88	O^{2-}
O3	1.07	OH^{-}
O4	1.85	O^{2-}
O5	1.67	O^{2-}
O6	1.73	O^{2-}
O7	1.78	O^{2-}
O8	1.93	O^{2-}
O37	0.27	H_2O

[a] The O atom is an O^{2-} if the BVS is ~1.8−2.0, an OH^{-} if it is ~1.0−1.2, and a H_2O if it is ~0.2−0.4, but the ranges can be affected by H bonding.

as a result of it acting as a double H-bond acceptor, for example, a BVS of 1.03 for an unequivocally O^{2-} ion H-bonding to two neighboring H_2O groups.[53] All of the Mn atoms are six-coordinate with distorted octahedral geometry; Mn2 and Mn5 are very distorted, with one JT elongated bond being particularly long (Mn2−O15 = 2.588(3) Å, Mn5−O13 = 2.522(3) Å). There are no significant intermolecular interactions.

The structure and a stereoview of $[Mn_{12}O_7(OH)(OMe)_2(O_2CPh)_{12}(dmhmp)_4(H_2O)]$ (**2**) are shown in Figure 2, and its labeled core in Figure S2 (Supporting Information). Selected interatomic distances and angles are listed in Table 5. The complex is mixed-valent $Mn^{II}_3Mn^{III}_9$, as indicated by the metric parameters and confirmed by BVS calculations (Table 3), and contains a $[Mn_{12}(\mu_4\text{-}O)_4(\mu_3\text{-}O)_5(\mu\text{-}O)_7]$ core consisting of a central $[Mn_4(\mu_4\text{-}O)_2(\mu_3\text{-}O)_4]$ face-sharing incomplete dicubane (Mn1, Mn2, Mn3, and Mn4), and on either side of this is attached a $[Mn_4(\mu_4\text{-}O)]$ tetrahedral unit. There is an interesting asymmetry in that the tetrahedral unit is $Mn^{II}Mn^{III}_3$ on one side and $Mn^{II}_2Mn^{III}_2$ on the other. BVS calculations were performed on the inorganic O atoms to assess their degree of protonation (Table 4), and there are four $\mu_4\text{-}O^{2-}$ (O1, O6, O7, and O8), three $\mu_3\text{-}O^{2-}$ (O2, O4, and O5), one $\mu_3\text{-}OH^{-}$ (O3), one $\mu_3\text{-}MeO^{-}$ (O38), one $\mu\text{-}MeO^{-}$ (O39), and four $\mu\text{-}RO^{-}$ alkoxide arms (O9, O10, O11, O12) of $\eta^1{:}\eta^2{:}\mu$-dmhmp^{-} groups, and a terminal water molecule (O37). Two additional μ-O atoms are provided by benzoate groups bridging in μ_3 modes (O22 and O16). Peripheral ligation is provided by 12 benzoate groups exhibiting four binding modes: eight bridge two Mn atoms in the common $\eta^1{:}\eta^1{:}\mu$ mode, two bridge three Mn atoms in the rarer $\eta^2{:}\eta^1{:}\mu_3$ mode, one chelates Mn^{II} atom Mn12, and one is terminally bound to Mn^{II} atom Mn6, with its inbound O atom (O30) statically disordered between forming a H bond to the nearby water (O37) (O30···O37 = 2.654(5) Å) or the $\mu_3\text{-}OH^{-}$ (O3) group (O30···O3 = 2.713(3) Å). The four dmhmp^{-} groups all bind in a $\eta^1{:}\eta^2{:}\mu$ mode. The Mn atoms are six-coordinate with distorted octahedral geometry, except for Mn11, which is five-coordinate unless a long sixth bond (Mn11−O24 = 2.842(3) Å is included. Again, there are no significant intermolecular interactions.

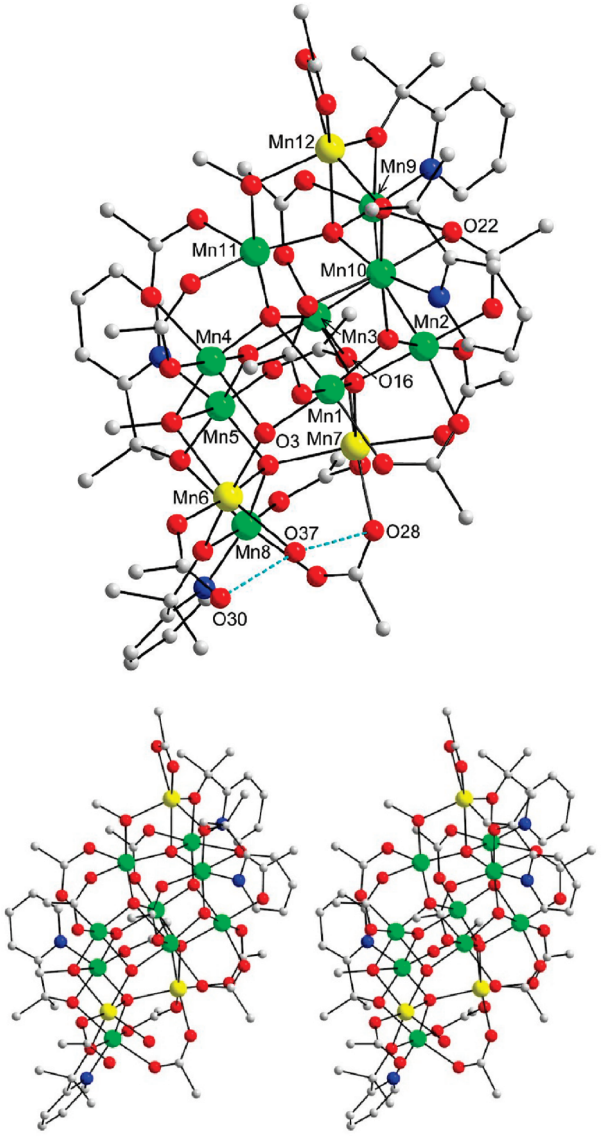

Figure 2. Structure of complex **2** with intramolecular H bonds shown as dashed lines (top) and a stereopair (bottom). Hydrogen atoms and benzoate Ph rings (except for ipso C atoms) have been omitted for clarity. Color code: Mn^{II}, yellow; Mn^{III}, green; O, red; C, gray; N, blue.

It is interesting to note that the Mn_x topologies of **1** and **2** are related, consisting of one (**1**) or two (**2**) $[Mn_4(\mu_4\text{-}O)]$ tetrahedral units attached to a second type of unit: in **1**, the latter is a $[Mn_3(\mu_3\text{-}O)]$ triangular unit (which forms a butterfly with one of the Mn atoms of the tetrahedral unit), whereas in **2**, it is two edge-sharing $[Mn_3(\mu_3\text{-}O)]$ triangular units (the core of the incomplete face-sharing dicubane).

It is also of interest that Mn_{12} benzoate complex **2** is similar to a reported Mn_{12} benzoate complex with hmp^{-}, $[Mn_{12}O_8Cl_4(O_2CPh)_8(hmp)_6]$ (**3**).[27b] Disregarding differences such as MeO^{-} in **2** versus Cl^{-} in **3**, and looking instead at the overall structures, the two complexes are

(53) Mishra, A.; Tasiopoulos, A. J.; Wernsdorfer, W.; Abboud, K. A.; Christou, G. *Inorg. Chem.* **2007**, *46*, 3105–3115.

Table 5. Selected Interatomic Distances (Å) for $2\cdot 3CH_2Cl_2$

Mn1−O4	1.880(3)	Mn7−O19	2.142(3)
Mn1−O1	1.918(3)	Mn7−O7	2.155(3)
Mn1−O3	1.930(3)	Mn7−O28	2.168(3)
Mn1−O23	1.960(3)	Mn7−O13	2.209(3)
Mn1−O33	2.214(3)	Mn7−O16	2.296(3)
Mn1−O6	2.343(3)	Mn7−O1	2.314(3)
Mn2−O4	1.902(3)	Mn8−O10	1.894(3)
Mn2−O20	1.942(3)	Mn8−O7	1.896(3)
Mn2−O1	1.958(3)	Mn8−O14	1.943(3)
Mn2−O21	1.974(3)	Mn8−N2	2.041(3)
Mn2−O34	2.140(3)	Mn8−O27	2.120(3)
Mn2−O5	2.165(3)	Mn8−O9	2.264(3)
Mn3−O5	1.866(3)	Mn9−O5	1.844(3)
Mn3−O2	1.901(3)	Mn9−O11	1.908(3)
Mn3−O17	1.973(3)	Mn9−O8	1.908(3)
Mn3−O1	2.004(3)	Mn9−N3	2.034(4)
Mn3−O16	2.205(3)	Mn9−O18	2.118(3)
Mn3−O6	2.251(3)	Mn9−O22	2.447(3)
Mn4−O2	1.880(3)	Mn10−O12	1.879(3)
Mn4−O6	1.890(3)	Mn10−O4	1.895(3)
Mn4−O38	1.942(3)	Mn10−O8	1.909(3)
Mn4−O35	1.988(3)	Mn10−N4	2.022(4)
Mn4−O25	2.153(3)	Mn10−O24	2.217(3)
Mn4−O3	2.302(3)	Mn10−O22	2.321(3)
Mn5−O2	1.879(3)	Mn11−O6	1.857(3)
Mn5−O9	1.883(3)	Mn11−O39	1.891(3)
Mn5−O7	1.905(3)	Mn11−O8	1.925(3)
Mn5−N1	2.038(3)	Mn11−O36	2.003(3)
Mn5−O15	2.231(3)	Mn11−O26	2.093(3)
Mn5−O38	2.387(3)	Mn12−O39	2.085(3)
Mn6−O29	2.129(3)	Mn12−O11	2.143(3)
Mn6−O10	2.130(3)	Mn12−O12	2.160(4)
Mn6−O3	2.170(3)	Mn12−O32	2.225(10)
Mn6−O37	2.226(3)	Mn12−O31	2.227(11)
Mn6−O7	2.264(3)	Mn12−O8	2.326(3)
Mn6−O38	2.284(3)		

similar in that both consist of a central face-sharing incomplete dicubane, on either side of which are two tetrahedral units attached to the oxide ions of the former. However, there is a major difference in that **3** is centrosymmetric, whereas **2** is unusually asymmetric, in both the distribution and binding modes of many ligands and in the Mn oxidation state distribution, being $[Mn^{II}{}_3Mn^{III}{}_9]$ in **2** and $[Mn^{II}{}_2Mn^{III}{}_{10}]$ in **3**. In both cases, however, the dmhmp$^-$ and hmp$^-$ groups are all bound in the same $\eta^1{:}\eta^2{:}\mu$ modes.

Magnetochemistry. Magnetic Susceptibility Study of Complex 1. Variable-temperature dc magnetic susceptibility measurements were performed on a microcrystalline powder sample of vacuum-dried **1**·MeCN in a 1 kG (0.1 T) field and in the 5.0−300 K range. The sample was restrained in eicosane to prevent torquing. The obtained data are shown as a $\chi_M T$ versus T plot in Figure 3. $\chi_M T$ gradually decreases from 16.22 $cm^3 K\ mol^{-1}$ at 300 K to 13.44 $cm^3\ K\ mol^{-1}$ at 25.0 K and then rapidly decreases to 10.11 $cm^3\ K\ mol^{-1}$ at 5.0 K. The 300 K value is much less than the spin-only ($g = 2$) value of 22.38 $cm^3\ K\ mol^{-1}$ for six Mn^{III} and one Mn^{II} noninteracting atom, indicating dominant antiferromagnetic exchange interactions. The plot does not appear to be heading to zero at 0 K, indicating that **1**·MeCN has an $S > 0$ ground state, and the 5 K value can be compared with the spin-only ($g = 2$) values of 7.88 $cm^3\ K\ mol^{-1}$ expected for an $S = 7/2$ state. To determine the ground state of **1**·MeCN, as well as the magnitude and sign of D, magnetization (M) versus dc field data were collected on restrained samples in the 1−7 T magnetic field (H) and 1.8−10.0 K temperature ranges. We attempted to fit the data, using the program MAGNET,[54] by diagonalization of the spin Hamiltonian matrix assuming only the ground state is populated, incorporating axial anisotropy ($D\hat{S}_z{}^2$) and Zeeman terms and employing a full powder average. The corresponding spin Hamiltonian is given by eq 3, where $\hat{S}_z$ is the easy-axis spin operator, g is the Landé g factor, μ_B is the Bohr magneton, and μ_0 is the vacuum permeability. However, we could not get an acceptable fit using data collected over the whole field range, which is a common problem caused by low-lying excited states, especially if some have an S value greater than that of the ground state. This conclusion is supported by the M versus H plot (Figure S3, Supporting Information), which does not show saturation but instead a steadily increasing magnetization with H. A common solution is to use only data collected at low fields (≤1.0 T), as we showed for many mixed-valence Mn^{II}/Mn^{III} clusters,[55] but for **1**·MeCN, it was still not possible to obtain a satisfactory fit assuming only the ground state is populated in this temperature range, suggesting particularly low-lying excited states. Thus, we turned to ac susceptibility measurements, which are a powerful complement to dc studies for determining the ground state of a system, because they preclude complications from a dc field.[9b,13a,43c]

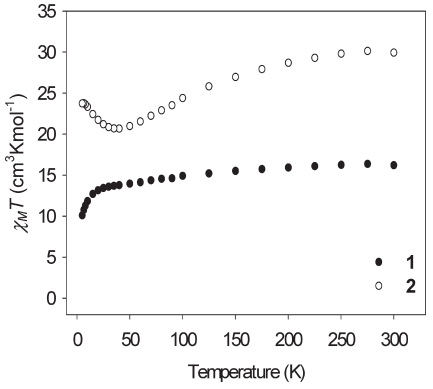

Figure 3. Plots of $\chi_M T$ versus T for complexes **1**·MeCN and $2\cdot 3H_2O$.

$$H = D\hat{S}_z^2 + g\mu_B\mu_0\hat{S}\cdot H \qquad (3)$$

The ac studies on **1**·MeCN were performed in the 1.8−15 K range using a 3.5 G ac field oscillating at frequencies in the 50−1000 Hz range. The obtained in-phase ac susceptibility data (χ_M', plotted as $\chi_M' T$) are shown in Figure 4. In the absence of slow magnetization relaxation and a resulting out-of-phase signal (χ_M''), the ac $\chi_M' T$ is equal to the dc $\chi_M T$, allowing determination of the ground state S in the absence of a dc field. The $\chi_M' T$ versus T plot of Figure 4 decreases significantly with decreasing temperature, indicating a population of one or more excited states with S greater than the ground state S, rationalizing the problematic fits of dc magnetization data. Extrapolation of the plot to 0 K, where only the ground state will be populated, gives a $\chi_M' T$ value of

(54) Davidson, E. R. *MAGNET*; Indiana University: Bloomington, IN, 1999.

(55) (a) Soler, M.; Wernsdorfer, W.; Folting, K.; Pink, M.; Christou, G. *J. Am. Chem. Soc.* **2004**, *126*, 2156. (b) King, P.; Wernsdorfer, W.; Abboud, K. A.; Christou, G. *Inorg. Chem.* **2005**, *44*, 8659.

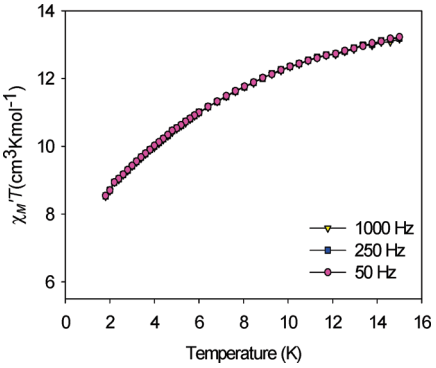

Figure 4. In-phase ac susceptibility (χ_M') signal, plotted as $\chi_M'T$ versus T, for complex **1**·MeCN in a 3.5 G field oscillating at the indicated frequencies.

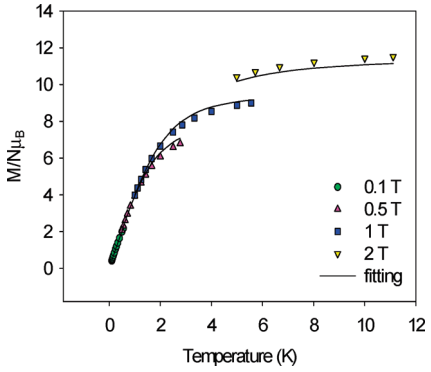

Figure 5. Plot of reduced magnetization ($M/N\mu_B$) versus H/T for complex **2**·3H$_2$O. The solid lines are the fits of the data; see the text for the fit parameters.

$\sim$7 cm^3 K mol^{-1}, which is the value expected for an S = 7/2 state, with g slightly less than 2 as expected for a Mn^{II}/Mn^{III} complex. Extrapolation of a steeply sloping plot to 0 K can be unreliable, especially for large S ground states and even in the absence of significant intermolecular interactions, but the data for **1**·MeCN clearly distinguish the S = 5/2, 7/2, and 9/2 possibilities, whose $\chi_M'T$ values are 4.38, 7.35, and 12.38 cm^3 K mol^{-1}, respectively, for g = 2. We thus feel confident in our conclusion that **1**·MeCN has an S = 7/2 ground state. Complex **1**·MeCN exhibited no out-of-phase (χ_M'') ac signal down to 1.8 K, indicating that it does not exhibit a significant barrier (versus kT) to magnetization relaxation, that is, it is not a SMM.

Magnetic Susceptibility Study of Complex 2. Variable-temperature dc magnetic susceptibility data for vacuum-dried complex **2**·3H$_2$O were collected as for **1**·MeCN and are shown as a $\chi_M T$ versus T plot in Figure 3. $\chi_M T$ gradually decreases from 29.94 cm^3 K mol^{-1} at 300 K to a minimum of 20.69 cm^3 K mol^{-1} at 40.0 K and then increases to 23.75 cm^3 K mol^{-1} at 5 K. The 300 K value is much less than the spin-only (g = 2) value of 40.13 cm^3 K mol^{-1} for three Mn^{II} and nine Mn^{III} noninteracting ions, indicating the presence of antiferromagnetic interactions, but the $\chi_M T$ versus T profile suggests there may also be significant ferromagnetic interactions as well. The 5.0 K value is indicative of an S = 13/2 ground state (expected $\chi_M T$ = 24.38 cm^3 K mol^{-1} for g = 2).

Magnetization data for **2**·3H$_2$O were collected at different fields and temperatures, as for **1**·MeCN, and attempts were made to fit them to eq 3. Again, we could not obtain a satisfactory fit using all data up to 7 T (Figure S4, Supporting Information), but this time we were able to get around the problem with excited states by using only data collected up to 2 T. These are shown as a reduced magnetization ($M/N\mu_B$) versus H/T plot in Figure 5, where N is Avogadro's number, and the fit (solid lines in Figure 5) gave S = 13/2, D = $-$0.18 cm^{-1}, and g = 1.97. Alternative fits with S = 11/2 or 15/2 were rejected because they gave unreasonable values of g. The root-mean-square D versus g error surface for the fit was generated using the program GRID[56] and is shown as a 2-D contour plot in Figure 6 for the D = $-$0.3 to + 0.3 cm^{-1} and g = 1.8$-$2.2 ranges. Two soft fitting minima

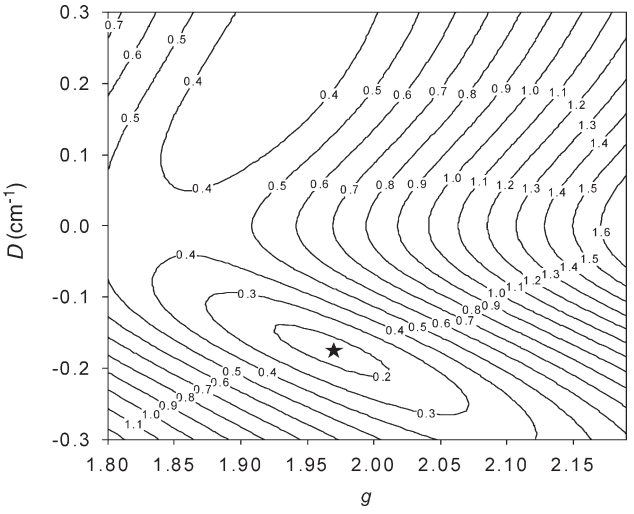

Figure 6. Two-dimensional contour plot of the root-mean-square error surface for the D versus g fit for complex **2**·3H$_2$O. The star marks the best-fit position.

are observed with positive and negative D values, with the latter being clearly superior and indicating D to be negative. From the shape and orientation of the contour describing the region of minimum error, we estimate the uncertainties in the fit parameters as S = 13/2, D = $-$0.18(2) cm^{-1}, and g = 1.95(2). Note that these are fit uncertainties, rather than an estimation of the accuracy of the obtained values.

The in-phase ($\chi'_M T$) and out-of-phase (χ''_M) ac susceptibilities for **2**·3H$_2$O are shown in Figure 7. $\chi_M'T$ increases with decreasing temperature below 15 K to a plateau of $\sim$24.5 cm^3 K mol^{-1} in the 4$-$5 K region and then exhibits a frequency-dependent decrease below 3 K. The plateau value is clearly indicative of an S = 13/2 ground state with $g \sim 2.0$, in agreement with the dc magnetization fit. S = 11/2 and 15/2 ground states would be expected to give $\chi_M'T$ values of 17.9 and 31.9 cm^3 K mol^{-1}, respectively, clearly very different from the experimental value. We conclude that complex **2**·3H$_2$O has an S = 13/2 ground state. The frequency-dependent decrease in $\chi_M'T$ below 3 K is accompanied by the appearance of frequency-dependent out-of-phase χ_M'' signals below 3 K, clearly the tails of peaks whose maxima are at $<$1.8 K. This is suggestive of the slow magnetization relaxation of a SMM.

(56) Davidson, E. R. *GRID*; Indiana University: Bloomington, IN, 1999.

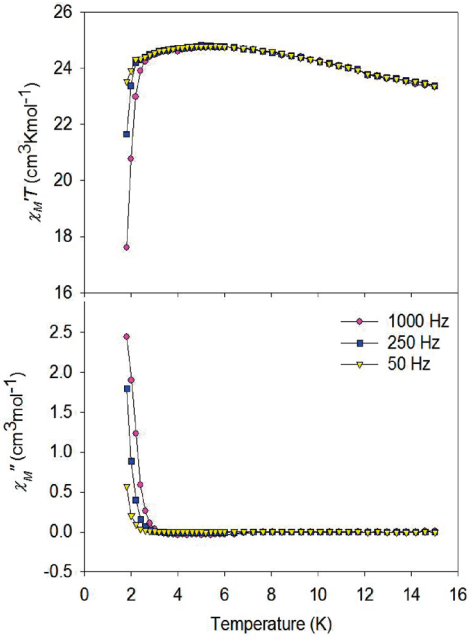

Figure 7. The ac susceptibility of complex $2\cdot 3H_2O$ in a 3.5 G field oscillating at the indicated frequencies: (top) in-phase (χ_M') signal plotted as $\chi_M'T$ versus T and (bottom) out-of-phase signal χ_M'' versus T.

To confirm whether $2\cdot 3H_2O$ is a SMM, studies were carried out on a single crystal down to 0.04 K.

Hysteresis Studies below 1.8 K. Magnetization versus applied dc field studies down to 0.04 K were carried out using a micro-SQUID on single crystals of $2\cdot 3CH_2Cl_2$ that had been kept in contact with their mother liquor.[57] Magnetization versus field hysteresis, the diagnostic property of a magnet, was observed below 0.7 K (Figure 8). The hysteresis loops exhibit increasing coercivity with increasing field sweep rate at a constant temperature (Figure S5, Supporting Information) and increasing coercivity with decreasing temperature at a constant sweep rate (Figure 8), as expected for the superparamagnet-like properties of a SMM. These loops thus confirm complex $2\cdot 3CH_2Cl_2$ to be a new addition to the family of SMMs.

The most dominating feature of the hysteresis loops in Figure 8 is the large step at zero field due to QTM through the anisotropy barrier. The large zero-field step indicates that QTM in zero field is fast, and this is consistent with the low symmetry of the molecule, which introduces a significant rhombic (transverse) anisotropy into the spin Hamiltonian, that is, $E(\hat{S}_x^2 - \hat{S}_y^2)$, where E is the rhombic zero-field splitting parameter. Of course, half-integer spin SMMs should not display QTM in the absence of transverse fields, but sources of the latter are provided primarily by the transverse components of dipolar fields from neighboring molecules, hyperfine interactions with the ^{55}Mn nuclear spins (I = 5/2, 100%), and intermolecular exchange coupling.[58] The greater is the transverse anisotropy, the greater will be the mixing of levels on either side of the anisotropy barrier, leading to increased

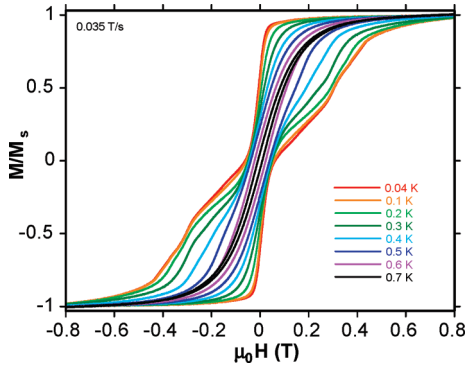

Figure 8. Magnetization (M) versus dc field hysteresis loops for a single crystal of $2\cdot 3CH_2Cl_2$ at the indicated temperatures and field sweep rate. The magnetization is normalized to its saturation value, M_S.

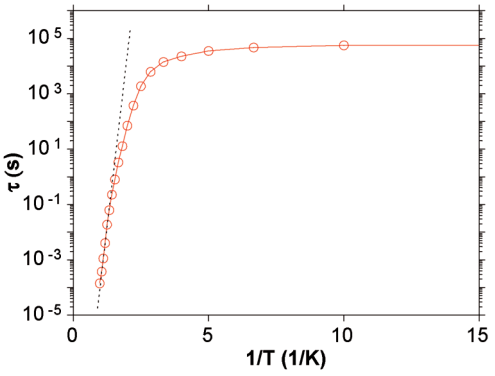

Figure 9. Arrhenius plot of the relaxation time (τ) versus $1/T$ for a single crystal of $2\cdot 3CH_2Cl_2$. The dashed line is the fit of the data in the thermally activated region to the Arrhenius equation; see the text for the fit parameters.

rates of QTM. In order to estimate the effective barrier (U_{eff}) to magnetization relaxation, the magnetization was first saturated in one direction at ~5 K with a large dc field, the temperature decreased to a chosen value, the field removed, and the magnetization decay monitored with time (Figure S6, Supporting Information). This provided magnetization relaxation time (τ) versus temperature data, shown as a τ versus $1/T$ plot in Figure 9 based on the Arrhenius relationship of eq 4:

$$\tau = \tau_0 \exp(U_{eff}/kT) \qquad (4)$$

where τ_0 is the pre-exponential factor and k is the Boltzmann constant. The fit of the thermally activated region above ~0.7 K (dashed line in Figure 9) gave U_{eff} = 11 cm^{-1} (16 K) and $\tau_0 = 2 \times 10^{-11}$ s. The small value of τ_0, smaller than is typical for purely SMM behavior, is likely due to low-lying excited states; larger clusters often give somewhat smaller τ_0 values, particularly for the latter reason.[59,60] It should also be noted that the kinetic U_{eff} value is slightly greater than the thermodynamic value (U) calculated to second order using $S^2|D|$ of U = 8(1) cm^{-1}. We assign this primarily to two reasons: (i) a greater intrinsic inaccuracy in the D value obtained from the magnetization

(57) Wernsdorfer, W. *Adv. Chem. Phys.* **2001**, *118*, 99.
(58) (a) Wernsdorfer, W.; Bhaduri, S.; Boskovic, C.; Christou, G.; Hendrickson, D. N. *Phys. Rev. B* **2002**, *65*, 180403. (b) Wernsdorfer, W.; Chakov, N. E.; Christou, G. *Phys. Rev. Lett.* **2005**, *95*, 037203.
(59) Murugesu; Takahashi, S.; Wilson, A.; Abboud, K. A.; Wernsdorfer, W.; Hill, S.; Christou, G. *Inorg. Chem.* **2008**, *47*, 4095 and references therein.
(60) Lampropoulos, C.; Hill, S.; Christou, G. *ChemPhysChem.* **2009**, *10*, 2397.

fit, which is reasonable given the problematic nature of low-lying excited states, and since the symmetry of complex **2**·$3CH_2Cl_2$ is much less than the axial assumed in the fitting model, and (ii) the contributions to the magnetization relaxation of pathways involving low-lying excited states, as we have reported recently elsewhere for $[Mn_{12}O_{12}(O_2CR)_{16}(H_2O)_4]$ complexes, giving an overestimation of U_{eff} and an abnormally small τ_0.[60]

Structural Comparison of hmp^-, $dmhmp^-$, and $dphmp^-$ Mn_x Products. Three related chelates based on the 2-(hydroxymethyl)pyridine (hmpH) backbone have now been explored in Mn cluster chemistry, hmpH itself and the dimethyl (dmhmpH) and diphenyl (dphmpH) derivatives (Scheme 1). In our previous report on dphmpH products, we concluded that the two Ph groups had almost completely removed the ability of the alkoxide O atom to bridge, and thus $dphmp^-$ primarily functions as a bidentate chelate. We rationalized this as a combination of the steric bulk of the two Ph groups, as well as their electron-withdrawing effect on the O atom. The choice of dmhmpH for the present work was designed to switch the bridging mode back on, as a result of both the smaller size of Me groups and their electron-donating rather than -withdrawing character, while still hopefully providing sufficient steric differences with hmp^- to lead to new products. This hope has been fulfilled, with $dmhmp^-$ acting as a perturbed hmp^-; that is, it functions as a chelating and bridging ligand, as does hmp^-, but it yields products **1** and **2** that are structurally distinct from any seen in Mn/hmp^- chemistry. Although the number of products containing $dmhmp^-$ is admittedly limited to date, it does appear that even the small Me substituents are sufficient to perturb the reactions to new cluster types compared with hmp^-.

Conclusions

We began this work asking whether the introduction of R groups at the CH_2 position next to the alkoxide O atom of hmp^- would provide routes to cluster types not available from hmp^- itself, and the answer is clearly "yes", both for previous work with dphmpH and the present work with dmhmpH. The initial use of the latter in Mn cluster chemistry has provided access to two new mixed-valence Mn_7 and Mn_{12} complexes **1** and **2** with unusually asymmetric structures not seen before, and with ground state spins of $S = 7/2$ and 13/2, respectively. In addition, **2** has proven to be a new SMM, as confirmed by single-crystal micro-SQUID studies. The combined results have shown that the addition of R groups next to the O atom of pyridyl-alcohols is a good way to modify the resulting cluster products, and that variation of the size and nature of the R groups provides a means of systematic modification of products, even though their exact structure cannot be predicted. We are currently extending this idea both to distinctly different R groups added to the hmp^- CH_2 position and to other alkoxide-containing chelating/bridging ligands, and results will be reported in due course.

Acknowledgment. We thank the National Science Foundation for support of this work through grants CHE-0414555 and CHE-0910472.

Supporting Information Available: X-ray crystallographic data in CIF format for complexes **1**·7MeCN and **2**·$3CH_2Cl_2$. This material is available free of charge via the Internet at http://pubs.acs.org.